Stoichiometry of Metabolite-Derived Particulate Organic Carbon and Nitrogen at Axial Seamount in the Northeastern Pacific Ocean

Ari Paulik

University of Washington

School of Oceanography

Seattle, WA

agpaulik@uw.edu

6/7/2026

Abstract

Hydrothermal vents support dense biological communities through the nutrients and minerals they provide to otherwise barren benthic environments. In this study, particulate organic carbon and nitrogen ratios were calculated from metabolite concentrations in water collected near two hydrothermal vents within Axial Seamount's caldera to assess differences in metabolite production and preferential nutrient uptake relative to samples taken at the chlorophyll maximum and deep sea. These ratios were also compared to the modernly accepted expected stoichiometry of 163C:22N (7.409), to determine how C:N ratios at hydrothermal vents compare to ratios expected in the surface ocean. A metabolomic analysis of the fifteen most abundant metabolites at each sampling site revealed four common metabolites in support of a core metabolism. However, unique metabolites were observed in addition to these commonalities, showing the distinctive biological processes essential to life at environmental extremes. C:N ratio analysis revealed significant carbon limitation and excessive nitrogen in sites that would be expected to have greater biological activity such as at the local chlorophyll maximum and near hydrothermal vents. These biologically dense sites each presented ratios indistinguishable from each other (4.62 and 4.37, respectively). The site at depth within the caldera and with no vent influence displayed a relatively higher ratio, confirming signals of preferential diets, energetic dynamics, and nutrient availability at hydrothermal vents. These findings establish that metabolite-derived C:N ratios at hydrothermal vent communities are comparable to those at the chlorophyll maximum, displaying how chemosynthetic and photosynthetic communities produce similar biological signals despite their extremely different nutrient sources.

Plain Language Summary

Located in the northeastern Pacific Ocean, Axial Seamount is a submarine volcano. Within its caldera are hydrothermal vent fields which release near-boiling seawater rich in nutrients and minerals into the water above. These fluids allow life specifically suited to exploit those extreme conditions to thrive. However, hydrothermal vents are inherently hard to study due to the limited and expensive technology able to travel to the seafloor and withstand the extreme conditions created by the deep ocean and vents. This has led to a poor understanding of the unique biology that lives near these vents compared to what is known about the easily accessible surface ocean. Within the surface ocean, marine microorganisms and molecules display a consistent average concentration of carbon and nitrogen, in a ratio of 163:22 (7.409). This ratio can be used to understand nutrient limitations and the preferential use of certain elements. This study applies this idea to samples taken from hydrothermal vents to understand the biological activity of vent life relative to life found at the surface. Metabolites were measured to inform this study, serving as evidence for the completion of biological processes. Some metabolites were shared amongst the extremely different environments studied, indicating there is a core metabolism shared amongst oceanic organisms, while some metabolites were unique to their sample site, demonstrating specific metabolic responses to survive the respective habitats. Additionally, C:N ratios calculated at 45m beneath the surface and at the hydrothermal vents were effectively the same, indicating a similar biological signal across these different communities. Finally, ratios differed enough between biologically active (below the surface and hydrothermal vent communities) and less active (deep communities with no vent influence) sites that show potentially different nutrient availability and preferential nutrient consumption across the sites. Through understanding nutrient availability in different regions of water, how organisms respond

to these nutrients through metabolite production, and their elemental ratio composition, this study provides a foundation for interpreting biological signals at hydrothermal vents relative to well-studied, expected surface ocean stoichiometric ratios.

Introduction

Characterized by Alfred Redfield, the Redfield ratio explains the concept that the elemental ratios of carbon, nitrogen, and other nutrients follow the stoichiometry of 106:16 in both particulate (>0.2µm including phytoplankton and bacteria) and dissolved (<0.2µm including nutrients and excreted metabolites) surface ocean pools (Redfield, 1934). This chemical observation is driven by the biological synthesis and decomposition of oceanic organic matter (Redfield, 1960). More recent research has revealed that the originally defined Redfield ratio may be an average of total observed datapoints with large margins of deviation dependent on characteristics such as life strategies, latitude, temperature, and nutrient supply (Geider & La Roche, 2002). It has been proposed that the modern elemental ratio is closer to 163:22 (Geider & La Roche, 2002; Martiny et al., 2014; Tanioka et al., 2022). Redfield ratio (referred to in this study as "historical stoichiometry") was based on relatively few samples taken in the 1930s. Over time, sampling resolution increased within the global surface ocean, leading to an increase in the overall average ratio to 7.409. Since this "modern stoichiometry" value of 163:22 (7.409) is seen in greater proportions today, this was the value used in this study. Variations in this ratio are ubiquitous; however, a significant deviation below or above expected stoichiometry can indicate nutrients in excess or limitation in biological systems dependent on the relative change in and between the elements. Given this research and ratio development, oceanic stoichiometry is well-understood in the surface ocean, with many studies defining how ratios shift with varying environmental conditions and life strategies (Chen et al., 1996; Hansell & Waterhouse, 1997; Martiny et al., 2014; Redfield, 1934; Redfield, 1960; Tanioka et al., 2022; Tett et al., 1985). In contrast, comparable research in the deep ocean is minimal. Through studying the stoichiometry of deep sea-dwelling chemoautotrophic communities relative to known biological ratios at the

surface, an understanding of what allows these novel life forms to thrive in their extreme environments can be developed, therefore expanding the knowledge of true global oceanic stoichiometric ratios.

Chemosynthetic bacterial and archaeal communities found in abundance near hydrothermal vents support the relatively small, but bountiful vent-bound food webs (Früh-Green et al., 2022). Hydrothermal vents form from cold seawater seeping into the long continuous fractures in oceanic basalt, traveling near subsurface magma chambers, heating up, becoming more buoyant, and dissolving surrounding metals before reaching a common orifice in the seabed (Früh-Green et al., 2022). The endmember fluids directly expelled from magmatic-dominated vents are known to be hot and acidic (commonly 6 to >400°C; pH 2-6; Table 1), but rapidly cool during entrainment with the surrounding seawater, precipitating minerals such as iron and sulfide to form chimneys surrounding the orifices. Other nutrients such as methane, nitrate, nitrite, and hydrogen sulfide expelled from the vents then becomes energetically available to the nearby microorganisms (Früh-Green et al., 2022).

Hydrothermal vents are found in highest abundance where tectonic plates separate through either divergence or back-arc spreading associated with convergence, naturally causing the basaltic seafloor to develop high permeability (Früh-Green et al., 2022). Located on the western Juan de Fuca plate spreading center, Axial Seamount is characterized as a divergent boundary, where the two proximal plates are moving away from one another (Fig. 1). Axial Seamount Hydrothermal Emissions Study (ASHES) is a hydrothermal vent field within Axial's caldera with hydrothermal processes dominated by lava flow rather than faulting (Hammond, 1990). The magma chambers below hydrothermal vents tend to be shallower along divergent boundaries relative to back-arcs, yielding endmember fluids that are hotter, putting relatively

more stress on the biology living there (Früh-Green et al., 2022). The two vents studied for this research at ASHES (Mushroom and Inferno) are among the hottest chimneys at Axial, with high CO_2 (low pH) content among other anomalous characteristics relative to the rest of the vent field (Butterfield et al., 1990).

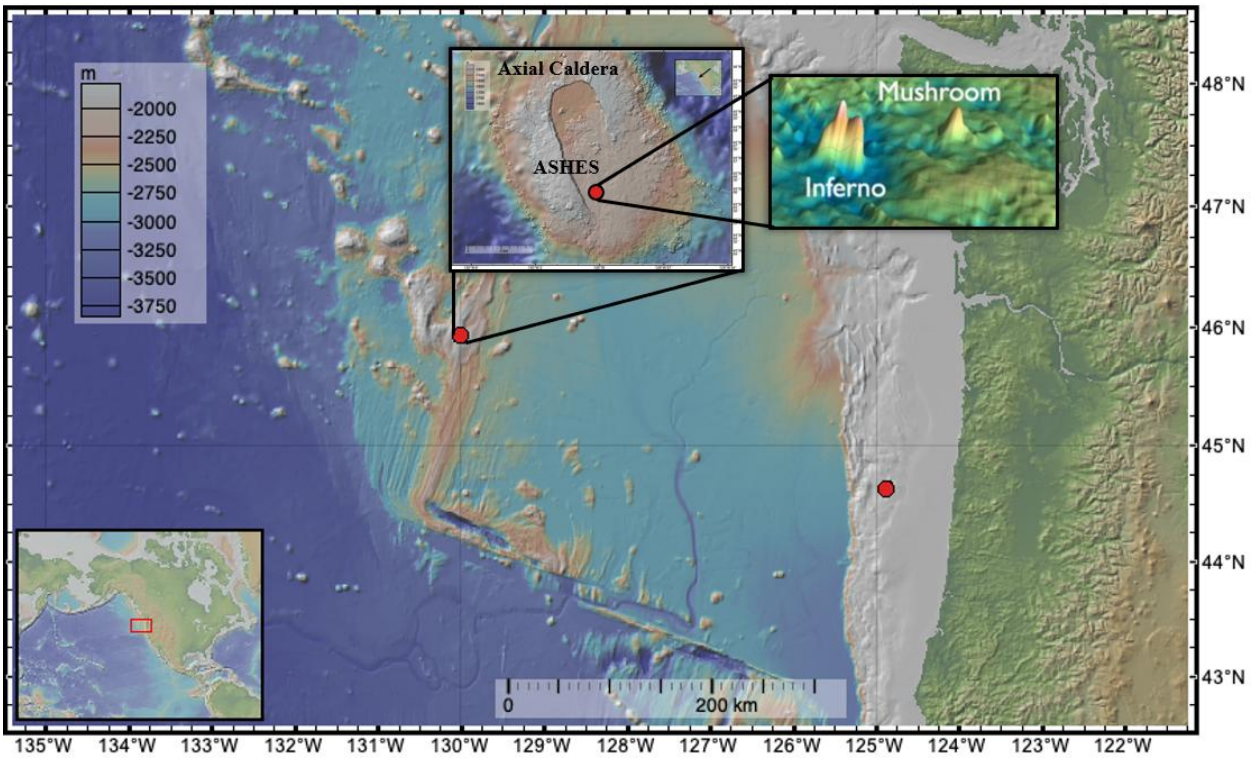

Figure 1. Map of the hydrothermal vents chosen for this study within one of Axial's caldera vent fields, ASHES. Each inset provides a higher resolution, high scale map of the sampling locations. Scale bars denote depth of features. Each grid mark in the inset showing Inferno and Mushroom is 2.6m. Red dot furthest to the right and closest to shore represents the Continental Shelf, 700m sample. Caldera and vent bathymetry inset referenced from Ocean Observatories Initiative's Regional Cabled Array.

Table 1. Endmember composition of hydrothermal vents used in this study compared to deep and surface water with no vent influence. Values expressed for deep and shallow water are approximate, as many exceptions are possible for values listed. Respective information compiled from each following source is noted with a letter superscript matched with the reference and its respective measurement: (Butterfield et al., 1990)[a], (Cadena et al., 2024)[b], (Früh-Green et al., 2022)[c], (NOAA Office of Satellite and Product Operations, 2026)[d], (NSF Ocean Observatories Initiative, 2014)[e], (NOAA Research, 2024)[f], (NOAA National Centers for Environmental Information, 2018)[g], (Park, 1966)[h], (Sieradzki et al., 2018)[i], (Wanninkhof et al., 2013)[j].

Characteristic	ASHES (Inferno and Mushroom)	Deep Water	Surface Water
Temperature	250-330°C[a]	~0-1.5°C[j]	~10-15°C[d]
pH	3.5[a]	≤7.9[h]	~8.05-8.1[f]
CO_2	50 mmol/kg[a]	~2.2 mmol/kg[c]	~2 mmol/kg[g]
Depth	1552m (caldera)[e]	Deep, near seabed	Near surface
Energy Production	Chemoautotrophy[c]	Heterotrophy[b]	Photoautotrophy[i]

Hydrothermal vents provide biologically essential nutrients such as iron, hydrogen sulfide, manganese, and cobalt to chemoautotrophic communities, surrounded by areas that are nutrient-poor in comparison (Früh-Green et al., 2022). This nutrient input allows for the use of sulfide in carbon fixation and chemoautotrophic energy production, allowing biological communities to grow (Früh-Green et al., 2022). Previous research has explored elemental ratios in few hydrothermal vent systems, such as those at the East Pacific Rise. Comita et al. (1984) found that particulate organic matter (POM) obtained near the vents chosen for the study differed from POM samples taken farther from those vents, with a C:N ratio decreasing by almost half, from 25 to 12, near the measured vent water. This finding continues to advance the understanding of elemental ratios in deep water, revealing invaluable information about the presence of biology at hydrothermal vents among a research field that has historically focused on the Redfield ratio in surface waters (Comita et al., 1984). Adding to this research, introducing additional vents into a similar analysis enhances understanding of how ratios vary by vent community, how metabolite-derived ratios compare to those of total POC/PN, and how they compare to local surface, highly productive waters. By filling these gaps in current hydrothermal research, this study enhances the understanding of how biological communities inhabiting vents produce metabolites necessary for survival in extreme environments, how these metabolites influence observed C:N ratios, and how these analyses compare to the deep and well-studied surface ocean.

This study aims to answer the question of how C:N ratios derived from particulate organic metabolites differ at hydrothermal vents relative to deep and surface water samples, as well as how these ratios compare to a global surface ocean expected stoichiometry. I hypothesized that metabolites synthesized in high concentrations would be almost entirely unique between sampling sites, analyzed by observing any overlap of each site's most abundant metabolites. Since metabolites are the by-products and intermediates for cellular metabolisms, they can be studied to understand the processes that are being performed within a biological community. Biology that is adapted to live at extreme pressures, without light, and near boiling waters is hypothesized to produce different metabolites relative to biological communities that are not subjected to these conditions. Second, I hypothesized that measured ratios in water adjacent to biologically dense vent walls will be statistically indistinguishable from modern elemental stoichiometry and/or the surface sample (chlorophyll maximum) collected above the vent. This is hypothesized because these chemoautotrophic communities may be provided with enough nutrients via hydrothermal venting to support similar signals of biological activity found near the surface, despite having different metabolic demands and processes. Anticipated biological activity shared between these environments includes processes such as carbon fixation allowed by the community's respective energy source, nutrient uptake, and metabolite production.

Methods

Sample collection at ASHES

To obtain particulate carbon and nitrogen ratios from the ASHES vent field (45° 55' 59.9"N, 130° 0' 50.4"W) in the Northeast Pacific Ocean, ROV *Jason* was deployed off R/V *Atlantis* in a series of dives from July 31st to August 31st, 2025. ROV *Jason* was equipped with two 5L Niskin bottles on its starboard side and lowered to approximately 1500m where it could collect seawater

samples within 12 inches of the sessile biological community fixed to the Mushroom and Inferno's chimneys. Two samples were taken from Inferno, one from the side with little suspended particulate matter (referred to as "Inferno, side 1") and another from the side with dense suspended particulate matter along the chimney wall (referred to as "Inferno, side 2"). One sample was taken from Mushroom. Two near seabed samples were taken to provide context for the level of productivity occurring in the deep ocean where an external nutrient supply, such as a hydrothermal vent, is not influencing nutrient availability. One of these near seabed samples was 40m away from Mushroom and Inferno, inside Axial Seamount's caldera, and another was outside of the caldera closer to the continental shelf (referred to as "caldera, 1500m" and "continental shelf, 700m", respectively) (Table 2).

Table 2. Descriptions of sample site names used in results, explaining the methods of sample collection for each site with respective depths provided.

Sample Site Name	**Sample Site Description**
45m below surface	Located at local chlorophyll maximum (45m)
Caldera, 1500m	Same depth as vent sites, 40m distance from vent within caldera (1537 m)
Continental Shelf, 700m	Closer to Oregon coast outside of caldera without vent influence (768 m)
Inferno, side 1	Within 12 inches of Inferno's chimney on side without notable suspended particulate matter (1537 m)
Mushroom	Within 12 inches of Mushroom's chimney (1538m)
Inferno, side 2	Within 12 inches of Inferno's chimney on side with notable suspended particulate matter (1536m)

Both non-vent sites are necessary to understand if differences seen in vent ratios are influenced by the vent, or by any specific conditions created within the caldera.

Niskin bottles fixed to a CTD rosette were lowered to 45m (chlorophyll maximum) to collect water samples from the surface to act as a reference. Once all samples were brought onboard, they were split into triplicate samples of 1-1.2L. Each sample was promptly processed onboard by filtration via JJ Biotek/COLE PARMER Masterflex L/S Standard Digital peristaltic pumps. All MasterFlex PharMed BPT Tubes were acid (HCl) cleaned ahead of processing and flushed with Milli-Q before, after, and in between each sample. Each seawater sample was filtered through 0.2µm PTFE filters to separate dissolved and particulate samples for further analyses to be done onshore. Blanks were collected by placing two filters within the same housing and processing the second filter in series. Following filtration, each filter was flash-frozen in liquid nitrogen and stored in a -80°C freezer until all samples reached the onshore laboratory at the University of Washington.

Processing of ASHES samples

Onshore, each filter was sonicated for five minutes to lyse cells. Metabolites were extracted using a modified lipid extraction and purification method using 1:1 methanol/water for the aqueous phase and dichloromethane for the organic phase (Bligh & Dyer, 1959). Samples were then separated through liquid chromatography using a HILIC column and measured using an Orbitrap Astral Mass Spectrometer (LC-MS). This process yielded the mass, charge, retention time, and peak area for each of the targeted metabolites in the particulate samples. The chromatogram output from the mass spectrometer was manually integrated using Skyline software (v.25.1). Quality control checks on the manual integrations and quantified concentrations of each metabolite in each sample were performed according to the Best-Matched Internal Standard Normalization methods (B-MIS) (Boysen et al., 2018). Some metabolites had concentrations just greater than 0nM, introducing uncertainty about whether the concentrations

of those metabolites were real or if it was random chance that their concentration was greater than 0nM. To account for this, a one-sided t-test using the standard mean error was performed for each metabolite per sample. Concentrations significantly greater than the respective blank ($p < 0.05$, $df = 2$) passed and had that blank concentration subtracted from the corresponding replicate environmental concentration. All metabolite concentrations that failed this test were considered below detection limit and quantified as 0nM. Molar C:N ratios were calculated at each site using the equation

$$(C:N)_{site} = \frac{\sum_{i=0}^{n}(C_i * [nM_i])}{\sum_{i=0}^{n}(N_i * [nM_i])}$$

where C_i and N_i denote the respective number of carbon and nitrogen atoms within the molecular structure of each metabolite and nM_i denotes the environmental concentration of the respective metabolite at each sampling site following the averaging across three technical replicates.

Sample collection at NW Rota-1

Located in the Northeast Pacific Ocean, water samples collected at NW Rota-1 (14° 36' 04"N, 144° 46' 30"E) were obtained aboard the R/V *Thomas G. Thompson* during March 22nd – March 31st, 2026, via Niskin bottles fixed to a CTD rosette. Samples were collected at the chlorophyll maximum depth (DCM; ~125m), 1650m along the vent's slope, and just above the vent's caldera at 415m. To find the appropriate location for hydrothermal vent sampling, bubbles were monitored on backscatter data coupled with multibeam SONAR to locate the plume of the vent. This was then compared with a depth sounder to understand where the CTD was in relation to the vent. Brown propylene bottles were rinsed 3 times with the water to be used for each sample to minimize cross-contamination. The samples were split into 960-1100mL triplicates and filtered through 25mm diameter, 0.2µm pore size GF/F filters (pre-combusted at 500°C for

4.5-5 hours) via a vacuum-based filtration system where the filters collected the entire particulate sample (all organisms caught on a 0.2µm filter). In addition to the environmental samples, there were also three procedural blanks conducted following the same process using deionized. This established how much of the signal seen in the experimental samples was from some level of inevitable carbon contamination during the filtration process. Filters were wrapped in a foil packet and frozen at -80°C to stop any biological activity from occurring while waiting for further processing on shore.

Processing of NW Rota-1 samples

At the University of Washington's Marine Chemistry Lab, samples were fumigated with HCl to remove any inorganic components. Using an Exeter Analytical CE 440 Elemental Analyzer, filters were each heated to 900-1000°C until the POC and PON transitioned to CO_2 and N_2, at which point their respective quantities were elementally analyzed through gas chromatography. Relative POC and PN values were output and calculated into an elemental ratio. These samples did not yield data usable within the timespan of this project; however, these methods can be used for future projects at alternate hydrothermal vents to contribute to the understanding of how geological processes such as plate tectonics may influence elemental ratios.

Data analysis

To statistically analyze the differences in ratios between sampling sites and compared to expected stoichiometry, t-tests, ANOVA, and Tukey Comparison of Means tests were conducted via R. A one-sample, two-sided t-test was performed at each sampling site (Table 2) to determine the presence of a significant relationship between each of the site's ratio and expected stoichiometry. The mean value utilized for this test was the average global ratio developed over

the last 40 years, or “modern stoichiometry” of 163:22 (7.409 divided). Statistical errors of conducting multiple t-tests do not accumulate in this case, as each resulting p-value will be interpreted independently. A one-way ANOVA test was conducted to determine statistical difference between sites, followed by a Tukey’s Comparison of Means test to determine which pairwise site comparisons were significantly different from each other. For all tests, a p-value less than 0.05 was ruled as statistically significant.

Results

Given the data used to produce these C:N ratios were obtained via metabolomic methods, it is necessary and helpful to understand these data before collapsing down into singular ratios averaged over each study site. Of the 98 metabolites targeted and of significant concentration in this study, 15 of the most abundant metabolites at each site were chosen for a small analysis (Fig. 3). 8 of those 15 abundant metabolites 45m below the surface were shared amongst the caldera at 700m and an average of the hydrothermal vent sites’ metabolite concentrations. 10 of the 15 of the most abundant metabolites within the caldera without vent influence were shared and 12 of the 15 of the hydrothermal vent abundant metabolites were shared amongst other sites (Fig. 3). However, differences exist between both the site’s relative concentrations of these common metabolites and the unique metabolites found at each site (Fig. 3).

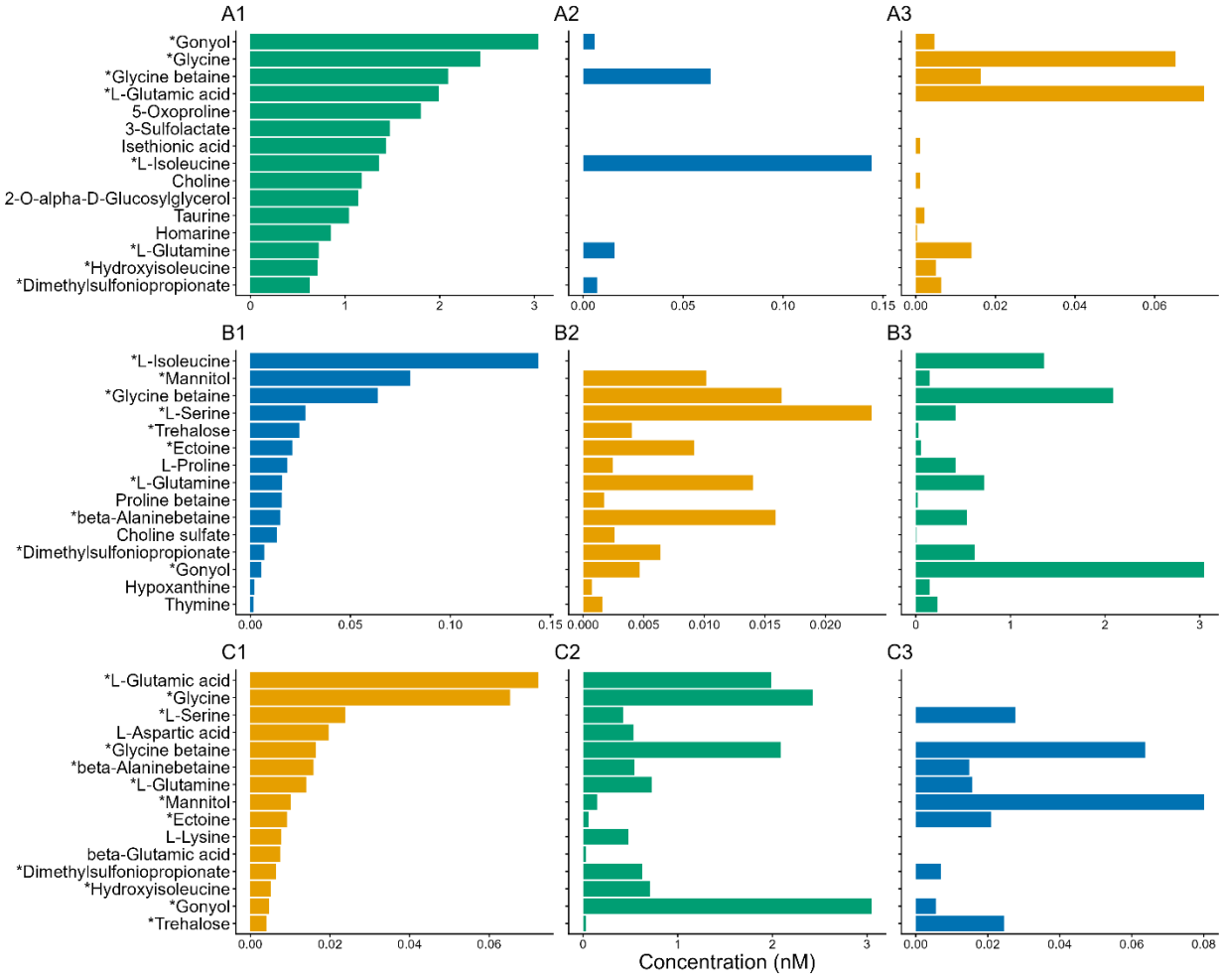

Figure 3. 15 most abundant particulate metabolites at 45m below surface (green), caldera at 1500m (blue), and an average of vent sites (yellow), displayed in column 1 (A1, B1, C1). Average of vent sites (yellow) was calculated by averaging each metabolite across each vent replicate, then across all vent sites (Inferno, side 1, Mushroom, and Inferno, side 2). Each row (A1, A2, and A3, for example) displays the same list of metabolites across each site, listed in the same order. This offers a visual comparison between the site displaying the concentrations of its most abundant metabolites with those same metabolites across the other sampling sites. Asterisks denote metabolites shared between at least one other sampling site. Gonyol, glycine betaine, dimethyl sulfoniopropionate, and L-glutamine are shared between all three sites. Three technical replicates per metabolite, per site were used to generate a mean, with a total mean generated across nine replicates and three sites for hydrothermal samples. Note the difference in axis scales for each panel.

These metabolites were used to derive C:N ratios for each of the sampling sites, which were then used to understand their significance in proximity to expected modern stoichiometry

(163:22; 7.409). The only site that was not statistically different from this expected mean was the caldera at 1500m (Table 3).

Table 3. The average carbon and nitrogen concentrations (nM) used to calculate C:N ratios at each sampling site. Each ratio was statistically analyzed against the modern stoichiometry value of 7.409 using independent, one-sample, two-sided t-tests (df = 2), yielding p-values that are labeled as significant with the (*) symbol.

Sample Site Name	Average Carbon Concentration (nM)	Average Nitrogen Concentration (nM)	C:N Ratio	p-value
45m below surface	205	44.5	4.62	3.00E-4*
Caldera, 1500m	3.30	0.537	6.24	5.55E-2
Continental Shelf, 700m	3.97	0.843	4.74	2.11E-3*
Inferno, side 1	1.26	0.269	4.69	1.17E-5*
Mushroom	1.64	0.342	4.80	3.28E-3*
Inferno, side 2	1.93	0.532	3.66	1.06E-3*

All other sites produced ratios significantly different from 7.409 (Table 3). The ratios lower than expected indicate either carbon limitation or excess nitrogen occurring at those respective sites (Fig. 4). When comparing site ratios to each other, Inferno, side 1 and Mushroom had ratios indistinguishable from each other, while Inferno, Side 2 had a ratio significantly lower than all other site ratios (Fig. 4). The caldera site at 1500m was statistically higher than all other site's ratios while the continental shelf site at 700m was indistinguishable from 45m below the surface, Inferno, side 1, and Mushroom (Fig. 4).

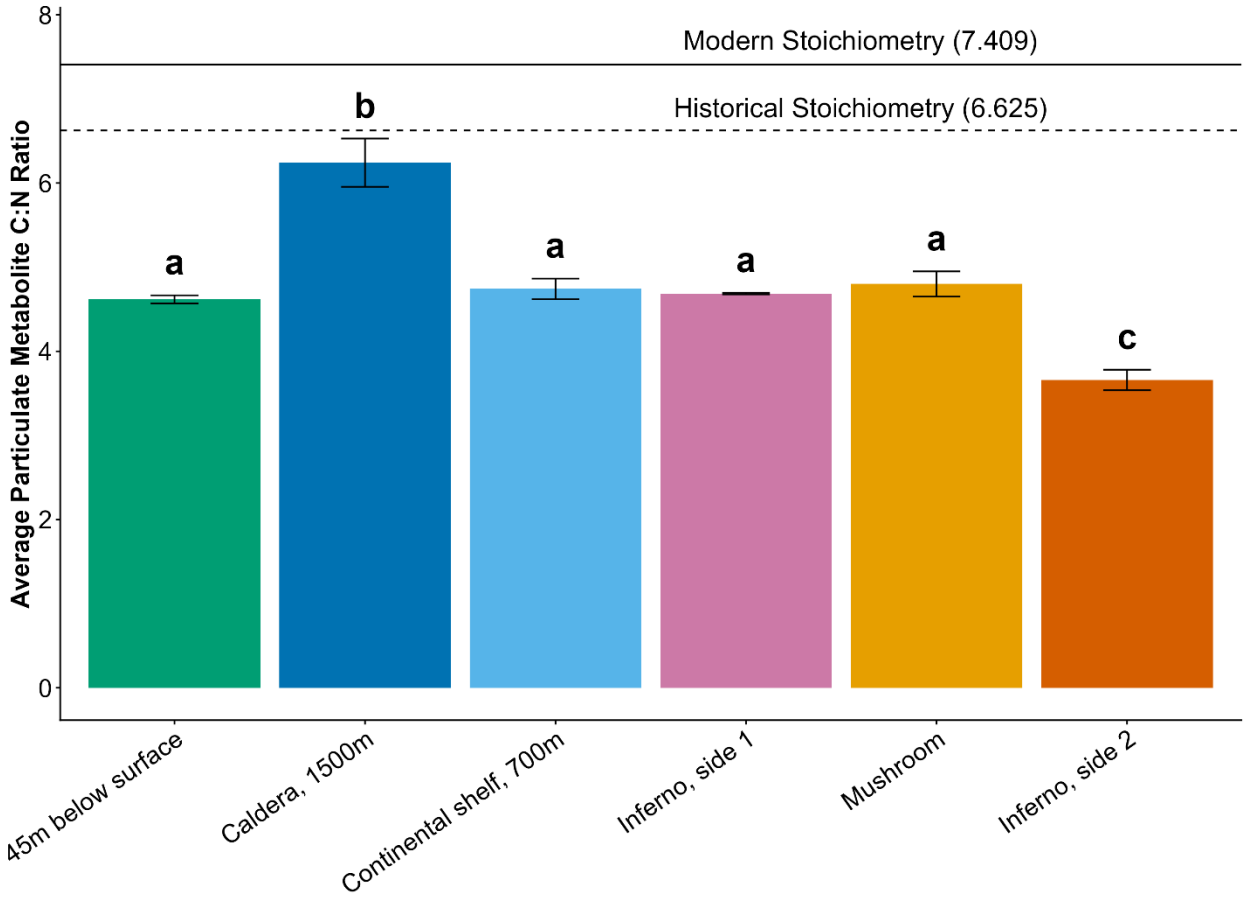

Figure 4. Metabolite-derived C:N ratios of the respective sampling sites with standard error bars (df=2). The historical stoichiometric value is denoted with a dashed line; the modern stoichiometric value is denoted with a solid black line. Letters above the bars indicate significance of ratios between sites based on a one-way ANOVA and Tukey Comparison of Means test.

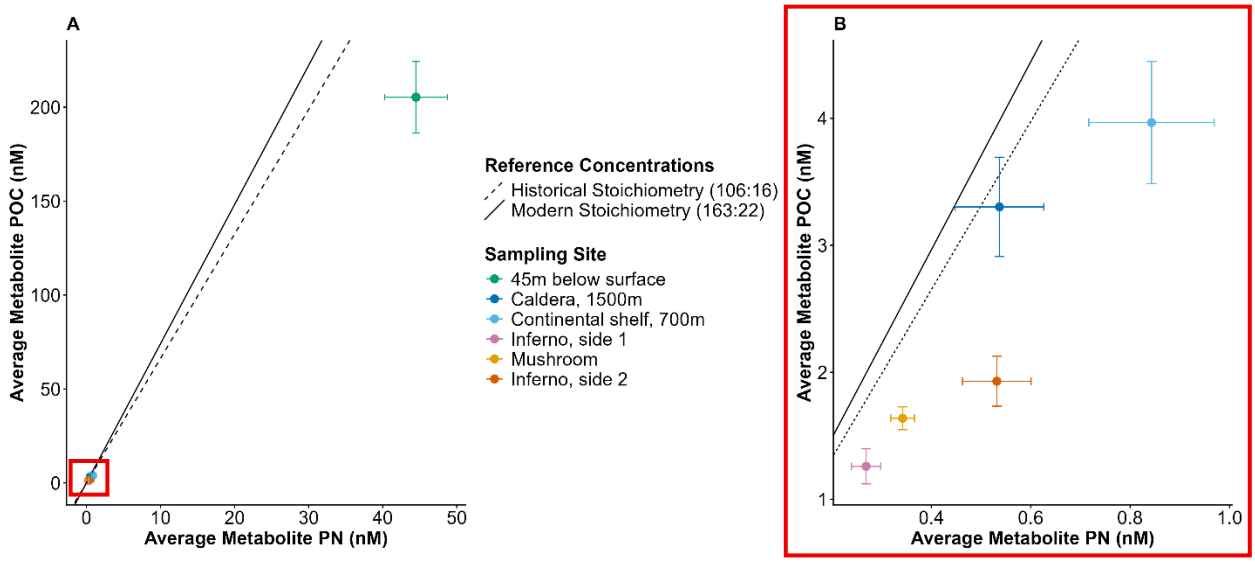

Figure 5. Average metabolite PN and POC of samples plotted against historical (dashed line) and modern (solid line) stoichiometries. Panel A shows all samples present on the same plot. Due to the low resolution of deep ocean samples in the presence of the 45m below surface site Panel B excludes this site and zooms in on the continental shelf at 700m, caldera at 1500m, and hydrothermal sites. Each point represents the mean of three replicates with error bars that denote standard error in both particulate organic carbon and nitrogen (df=2). Note the change in scale between the two panels.

A direct comparison of PN to POC is beneficial in understanding how each site's relative carbon and nitrogen concentrations contribute to the value of the ratio relative to expected stoichiometry (Fig. 5). A deviation from the slope of expected stoichiometry in this comparison indicates a difference in elemental concentrations significantly different from this expected stoichiometry. A ratio greater than expected stoichiometry would indicate carbon in excess and/or nitrogen limitation while a ratio below expected stoichiometry would indicate carbon limitation and/or nitrogen in excess. This difference can be compared across study sites to analyze and understand the relative carbon and nitrogen concentrations contributing to the creation of each ratio value.

Discussion

Strong similarities and differences in metabolites observed between sampling sites

This study analyzed 98 metabolites, adding to a smaller list of previously quantified dissolved metabolites from hydrothermal fluids sampled in the 9° N East Pacific Rise (Longnecker et al., 2018). This long target list yielded large overlap between abundant metabolites with 53-73% of each site's fifteen most abundant metabolites overlapping with at least one other site (not considering their respective concentrations), with four of those fifteen metabolites present in sites 45m below the surface, near the caldera bed, and the hydrothermal vents. While the concentrations of these metabolites differ between sites, this suggests that each of the communities represented at each site requires a core metabolic process expressed by the same core metabolites to survive in the ocean, despite living in extremely different environments. Metabolites shared between all sites chosen for this study include gonyol and dimethyl sulfoniopropionate (DMSP) which are both sulfonium reactants for dimethyl sulfide (DMS) production, glycine betaine which is a ubiquitous osmolyte, and L-glutamine which is an amino acid necessary for growth (Moran et al., 2022; Ngugi et al., 2020; Yoo et al., 2020). These metabolites are vital for nutrient cycling, regulating internal salinity, and growth and cell division, supporting the idea that shared metabolites between environmental extremes presented in this study are necessary to support a core metabolism and general life in the ocean (Moran et al., 2022; Ngugi et al., 2020; Yoo et al., 2020).

Despite these similarities, there are also observable differences among metabolites, unique to each of the sampling sites. Each of the most abundant, unique metabolites to each sampling site are amino acids, with 5-oxoproline found to be abundant 45m below the surface, L-Proline abundant in the caldera at 1500m, and L-aspartic acid abundant at hydrothermal vents (Kellock et al., 2020; Kumar & Bachhawat, 2012; Takasu & Nagata, 2015). While each of these are amino acids, they differ between each other based on processes they are a part of, supporting

the concept that unique metabolites are needed to foster unique biological communities found between these sites. This is expected, as biological communities with conditions such as access to solar energy, low pressure, and relatively warm temperature environments are likely to require different biological pathways and processes to survive compared to environments that require chemoautotrophy for carbon fixation. Since metabolites are small biological molecules used to communicate and maintain cell processes, unique abundant metabolites at each site exemplifies that there are different biological pathways being used at varying intensities in distinct environmental conditions, in conjunction with the core metabolisms defined by metabolites found at all sites (Johnson et al., 2016). This finding aligns with the original hypothesis that abundant metabolites observed between sites would be different, as well as with current research which has characterized significant differences in communities such as prokaryotes at shallow and deep depths through use of 16S rRNA and untargeted metabolomics (Steffen et al., 2022). Other studies have defined the biological communities between individual vents statistically different through use of terminal restriction fragment length polymorphism (TRFLP) and 16S rRNA (Fortunato et al., 2018; Huber et al., 2007; Opatkiewicz et al., 2009). These findings provide context for the unique metabolites found in different environments at different depths, despite using alternate methods. This knowledge of metabolite presence and abundance coupled with sampling site C:N ratios highlight the necessity for metabolite synthesis specifically adapted to the environments these biological communities live in, while still maintaining similarities to support general oceanic life.

Relationships of ratios between sampling sites

C:N ratios expressed at 45m below the surface, the local chlorophyll maximum, and at all hydrothermal vent samples except Inferno, side 2 were statistically indistinguishable from each

other, indicating similar signals of biological activity occurring at these environmental extremes. This finding supports the initial hypothesis that vents supply enough bioavailable nutrients and minerals to deep biological communities that a similar signal in biological activity is observable at the chlorophyll maximum. One observation that contrasted what was hypothesized was the continental shelf sampling site at 700m without vent influence displaying a C:N ratio indistinguishable from the hydrothermal vent sites (Inferno, side 1 and Mushroom). This may be due to changing nutrient regimes in proximity to land. Given this sample was taken at a relatively shallower depth and approximately 90km offshore (compared to ~500km offshore at ASHES), it is likely that this location experiences enhanced terrestrial nutrient influence and deep ocean mixing, potentially increasing nutrient supply at depth relative to more offshore sites that were part of this study (Cavender-Bares et al., 2001). However, a distinct hydrothermal signal was still observable as the C:N ratio at the caldera site at 1500m was distinguishable from all other sampling sites, due to its ratio similar to modern stoichiometry, compared to the more biologically active sampling sites of 45m and hydrothermal vents with significantly decreased ratios. The most likely reason for this relationship is the preferential remineralization of nitrogen-rich organic matter displayed by marine microbes (Hach et al., 2020). As surface organisms preferentially take up nitrogen-rich organic matter, deep ocean organisms are forced to fix carbon and obtain energy through a relatively higher amount of the harder-to-breakdown, carbon-rich organic and detrital matter that has sunk to depth (Hach et al., 2020). This uptake of high-carbon organic matter into deep, non-vent communities would be reflected in the produced metabolites, therefore yielding the higher elemental ratios observed at these sites. Contrastingly, hydrothermal vents may supply sufficient nitrogen to nearby biological communities that they are able to preferentially uptake these nutrients and present metabolite ratios like those observed at 45m

below the surface. Further, side 2 of Inferno had a ratio significantly lower than the other hydrothermal vent sites and 45m below the surface, likely due to the high concentration of particulate suspended matter near the vent wall, which was potentially indicative of enhanced nutrient delivery to communities on that side of Inferno. Since organisms that can exploit more nitrogen-rich resources can produce metabolites that contain more nitrogen and vice versa, this offers an explanation as to why the ratios produced between sampling sites show the signals of differing biological activity between expectedly productive and less productive waters.

Ratios below expected stoichiometry suggests excess and/or limiting nutrients

All sampling sites except the caldera at 1500m were statistically different from modern stoichiometry (163/22; 7.409), and all ratios fell below the global surface oceanic mean of 7.409. This indicates carbon limitation and/or nitrogen in excess at these sites. The data collected for this study cannot be used to confidently, mathematically conclude if carbon limitation or excess nitrogen is driving the reduced ratios, as both conditions could produce a ratio lower than expected. Analysis of a POC and PN plot can aid in visualizing which element may be driving the value of a ratio relative to other ratios. For example, side 2 of Inferno has a disproportionately higher nitrogen concentration than Mushroom, yet not much more carbon, indicating nitrogen in excess. However, this method is less effective for ratios that do not have other references around the slope of the expected stoichiometric values, leading to an inability to defensibly conclude which element drives the value of the ratio in some cases. A likely explanation for lower-than-expected ratios is the nutrient availability at each of the sampling sites, the preferential diet that occurs as a result, and the elemental ratio of metabolites that reflects preferential nutrient uptake. For example, the elemental ratio of the caldera site at 1500m may be significantly higher than the vent's ratios because these organisms living without an

autotrophic source rely on sinking carbon-rich molecules for carbon fixation and energy, whereas vents support life through the supply of nutrients and electron donors, fostering a community that is able to overpower the signals of sinking detritus through nitrogen uptake and metabolite synthesis. However, more research is needed to quantify this relationship and determine nutrient limitations or excess abundance.

Future endeavors

These findings contribute to the discovery of the metabolomes of hydrothermal vents, how they compare to the surface and deep ocean, and how they inform carbon and nitrogen stoichiometry in these extremely different environments. Characterizing these properties at depth and near hydrothermal vents helps inform how these understudied regions relate to the surface ocean, furthering our understanding of the similarities and differences held within the biology and processes required to inhabit the various layers of the water column.

To enhance this research, factors such as additional essential elements, nutrients, comparisons to total POC:PN, and analysis of metabolomic data at other hydrothermal vents and water parcels should be conducted. The Redfield ratio contains many other elements essential to life such as phosphorus and iron. Studying the ratios of these additional elements would provide more information on nutrient uptake, supply, and use across various environments. Analyzing changes in nutrient regimes at sites that are sampled to produce metabolite concentrations/elemental ratios can help inform how changes in nutrients such as phosphate and nitrate control these factors. For example, it would be expected that in areas with higher nutrient availability, biological communities would be plentiful and potentially carbon limited due to the high availability of nitrogen and phosphorus, elements which otherwise tend to be considered limiting. These abundant communities would therefore produce greater concentrations of

metabolites and produce a low elemental ratio. If a correlation such as this can be built, nutrients could help act as an indicator for metabolite concentrations and elemental ratios. Little research has been done characterizing how metabolite C:N ratios relate to total POC:PN. Since metabolites can be understood as evidence for life and its necessary processes, it is expected that metabolites follow a similar ratio as that of Redfield, but this has not been characterized and is important to understand for the future of interpreting analyses like those presented in this study. Additionally, it is important to conduct these analyses on other hydrothermal vents and water parcels throughout the water column to understand the deviation that occurs in elemental ratios that are derived from metabolites and how this compares with the deviation observed in the Redfield ratio. This provides information on how closely metabolites follow expected stoichiometry.

Conclusion

The goal of this study was to define the metabolomics and subsequent elemental ratios of carbon and nitrogen at two hydrothermal vents located along a divergent boundary and compare these ratios to well-studied, well-developed surface stoichiometries. The study of elemental ratios obtained through metabolomic methods of deep sea and hydrothermal vent sites has been neglected relative to similar studies in the surface ocean. To enhance the understanding of the deep ocean, its unique geological features, and the biological communities that inhabit them, it is important to characterize how active biology can be near vents in reference to surface and deep parcels, and how they are able to sustain this life. I hypothesized that metabolite abundances would be unique across sampling sites, and subsequent C:N ratios measured at hydrothermal vents (Inferno and Mushroom) would not be significantly different from expected stoichiometry since vents provide many of the needed nutrients and energetic constituents needed to support

the dense biology observed surrounding the chimneys. Several metabolites were seen in each of the environments despite their extremely different conditions, indicating a shared metabolism and processes that are generally necessary for oceanic survival. However, many abundant metabolites measured at each site were unique, showing that there are specific processes necessary for adaptation to environmental extremes. The condensation of this metabolomic data into C:N ratios displayed two of three vent samples that were significantly different from expected stoichiometry yet were indistinguishable from samples taken 45m below the surface at the local chlorophyll maximum indicating similar signals of biological activity between the sites. It was unexpected that the sampling sites 45m below the surface and hydrothermal vents display the lowest ratios, indicative of carbon limitation or excess nitrogen. This is likely a consequence of nutrient availability and preferential uptake of nitrogen-rich organic matter in contrast with non-vent sites that are subject to more carbon-rich organic matter, leading to a higher ratio.

To further this understanding of biological communities inhabiting hydrothermal vents, future studies should investigate a larger breadth of elements including iron and phosphorus to enhance knowledge of nutrient limitation, total POC and PN to assess if measuring a total value rather than metabolites changes the results seen in this study, and nutrient concentrations in relation to elemental ratios to understand how changes in nutrient regimes correspond to shift in ratios at hydrothermal vents.

Acknowledgements

Thank you to Lacie Levy, Jodi Young, the Thermal Extreme Autotrophy Lab, Ginger Armbrust, and Francois Ribalet for the guidance and mentorship, the captain and crew of the R/V *Atlantis* and R/V *Thomas G. Thompson*, the ROV *Jason* team, the Chief Scientists of VISIONS ‘25, Deborah Kelley and Katie Bigham, for facilitating sample collection and the Chief Scientist of the Senior Thesis Cruise ’26, Randie Bundy, for the endless support and planning before, during, and after this cruise. This work is supported by the National Science Foundation, Ocean Observatory Initiative’s Regional Cabled Array, and the School of Oceanography at the University of Washington.

Statement of Use of Artificial Intelligence

AI was used in the process of writing this proposal for small and infrequent suggestions on sentence restructuring and variations of wording. All output from AI was evaluated to ensure my words were still present and highlighted before suggestions were integrated into writing. Additionally, AI was used in the process of figure creation/coding. All output from AI was again, checked for correctness and relevancy to ensure my contributions and overall ideas were preserved.

References

Bligh, E. G., & Dyer, W. J. (1959). A rapid method of total lipid extraction and purification. *Canadian Journal of Biochemistry and Physiology*, *37*(8), 911–917. https://doi.org/10.1139/o59-099

Boysen, A. K., Heal, K. R., Carlson, L. T., & Ingalls, A. E. (2018). Best-Matched Internal Standard Normalization in Liquid Chromatography–Mass Spectrometry Metabolomics Applied to Environmental Samples. *Analytical Chemistry*, *90*(2), 1363–1369. https://doi.org/10.1021/acs.analchem.7b04400

Butterfield, D. A., Massoth, G. J., McDuff, R. E., Lupton, J. E., & Lilley, M. D. (1990). Geochemistry of hydrothermal fluids from Axial Seamount hydrothermal emissions study vent field, Juan de Fuca Ridge: Subseafloor boiling and subsequent fluid-rock interaction. *Journal of Geophysical Research: Solid Earth*, *95*(B8), 12895–12921. https://doi.org/10.1029/JB095iB08p12895

Cadena, L. R., Edgcomb, V., & Lukeš, J. (2024). Gazing into the abyss: A glimpse into the diversity, distribution, and behaviour of heterotrophic protists from the deep-sea floor. *Environmental Microbiology*, *26*(3), e16598. https://doi.org/10.1111/1462-2920.16598

Cavender-Bares, K. K., Karl, D. M., & Chisholm, S. W. (2001). Nutrient gradients in the western North Atlantic Ocean: Relationship to microbial community structure and comparison to patterns in the Pacific Ocean. *Deep Sea Research Part I: Oceanographic Research Papers*, *48*(11), 2373–2395. https://doi.org/10.1016/S0967-0637(01)00027-9

Chen, C.-T. A., Lin, C.-M., Huang, B.-T., & Chang, L.-F. (1996). Stoichiometry of carbon, hydrogen, nitrogen, sulfur and oxygen in the particulate matter of the western North

Pacific marginal seas. *Marine Chemistry*, *54*(1), 179–190. https://doi.org/10.1016/0304-4203(96)00021-7

Comita, P. B., Gagosian, R. B., & Williams, P. M. (1984). Suspended particulate organic material from hydrothermal vent waters at 21° N. *Nature*, *307*(5950), 450–453. https://doi.org/10.1038/307450a0

Fortunato, C. S., Larson, B., Butterfield, D. A., & Huber, J. A. (2018). Spatially distinct, temporally stable microbial populations mediate biogeochemical cycling at and below the seafloor in hydrothermal vent fluids. *Environmental Microbiology*, *20*(2), 769–784. https://doi.org/10.1111/1462-2920.14011

Früh-Green, G. L., Kelley, D. S., Lilley, M. D., Cannat, M., Chavagnac, V., & Baross, J. A. (2022). Diversity of magmatism, hydrothermal processes and microbial interactions at mid-ocean ridges. *Nature Reviews Earth & Environment*, *3*(12), 852–871. https://doi.org/10.1038/s43017-022-00364-y

Geider, R., & La Roche, J. (2002). Redfield revisited: Variability of C:N:P in marine microalgae and its biochemical basis. *European Journal of Phycology*, *37*(1), 1–17. https://doi.org/10.1017/S0967026201003456

Hach, P. F., Marchant, H. K., Krupke, A., Riedel, T., Meier, D. V., Lavik, G., Holtappels, M., Dittmar, T., & Kuypers, M. M. M. (2020). Rapid microbial diversification of dissolved organic matter in oceanic surface waters leads to carbon sequestration. *Scientific Reports*, *10*(1), 13025. https://doi.org/10.1038/s41598-020-69930-y

Hammond, S. R. (1990). Relationships between lava types, seafloor morphology, and the occurrence of hydrothermal venting in the ASHES Vent Field of Axial Volcano. *Journal*

of Geophysical Research: Solid Earth, *95*(B8), 12875–12893. https://doi.org/10.1029/JB095iB08p12875

Hansell, D. A., & Waterhouse, T. Y. (1997). Controls on the distributions of organic carbon and nitrogen in the eastern Pacific Ocean. *Deep Sea Research Part I: Oceanographic Research Papers*, *44*(5), 843–857. https://doi.org/10.1016/S0967-0637(96)00128-8

Huber, J. A., Mark Welch, D. B., Morrison, H. G., Huse, S. M., Neal, P. R., Butterfield, D. A., & Sogin, M. L. (2007). Microbial population structures in the deep marine biosphere. *Science (New York, N.Y.)*, *318*(5847), 97–100. https://doi.org/10.1126/science.1146689

Johnson, C. H., Ivanisevic, J., & Siuzdak, G. (2016). Metabolomics: Beyond biomarkers and towards mechanisms. *Nature Reviews Molecular Cell Biology*, *17*(7), 451–459. https://doi.org/10.1038/nrm.2016.25

Kellock, C., Cole, C., Penkman, K., Evans, D., Kröger, R., Hintz, C., Hintz, K., Finch, A., & Allison, N. (2020). The role of aspartic acid in reducing coral calcification under ocean acidification conditions. *Scientific Reports*, *10*(1), 12797. https://doi.org/10.1038/s41598-020-69556-0

Kumar, A., & Bachhawat, A. K. (2012). Pyroglutamic acid: throwing light on a lightly studied metabolite. *Current Science*, *102*(2), 288–297. http://www.jstor.org/stable/24083854

Longnecker, K., Sievert, S. M., Sylva, S. P., Seewald, J. S., & Kujawinski, E. B. (2018). Dissolved organic carbon compounds in deep-sea hydrothermal vent fluids from the East Pacific Rise at 9°50′N. *Organic Geochemistry*, *125*, 41–49. https://doi.org/10.1016/j.orggeochem.2018.08.004

Martiny, A. C., Vrugt, J. A., & Lomas, M. W. (2014). Concentrations and ratios of particulate organic carbon, nitrogen, and phosphorus in the global ocean. *Scientific Data*, *1*(1), 140048. https://doi.org/10.1038/sdata.2014.48

Moran, M. A., Kujawinski, E. B., Schroer, W. F., Amin, S. A., Bates, N. R., Bertrand, E. M., Braakman, R., Brown, C. T., Covert, M. W., Doney, S. C., Dyhrman, S. T., Edison, A. S., Eren, A. M., Levine, N. M., Li, L., Ross, A. C., Saito, M. A., Santoro, A. E., Segrè, D., … Vardi, A. (2022). Microbial metabolites in the marine carbon cycle. *Nature Microbiology*, *7*(4), 508–523. https://doi.org/10.1038/s41564-022-01090-3

Ngugi, D. K., Ziegler, M., Duarte, C. M., & Voolstra, C. R. (2020). Genomic Blueprint of Glycine Betaine Metabolism in Coral Metaorganisms and Their Contribution to Reef Nitrogen Budgets. *iScience*, *23*(5), 101120. https://doi.org/https://doi.org/10.1016/j.isci.2020.101120

Opatkiewicz, A. D., Butterfield, D. A., & Baross, J. A. (2009). Individual hydrothermal vents at Axial Seamount harbor distinct subseafloor microbial communities. *FEMS Microbiology Ecology*, *70*(3), 413–424. https://doi.org/10.1111/j.1574-6941.2009.00747.x

Park, K. (1966). Deep-Sea *p*H. *Science*, *154*(3756), 1540–1542. https://doi.org/10.1126/science.154.3756.1540

Redfield, A. C. (1934). *On the Proportions of Organic Derivatives in Sea Water and Their Relation to the Composition of Plankton*. University Press of Liverpool. https://books.google.com/books?id=szAezQEACAAJ

Redfield, A. C. (1960). The biological control of chemical factors in the environment. *Science Progress*, *11*, 150–170.

Sieradzki, E. T., Fuhrman, J. A., Rivero-Calle, S., & Gómez-Consarnau, L. (2018). Proteorhodopsins dominate the expression of phototrophic mechanisms in seasonal and dynamic marine picoplankton communities. *PeerJ*, *6*, e5798. https://doi.org/10.7717/peerj.5798

Steffen, K., Indraningrat, A. A. G., Erngren, I., Haglöf, J., Becking, L. E., Smidt, H., Yashayaev, I., Kenchington, E., Pettersson, C., Cárdenas, P., & Sipkema, D. (2022). Oceanographic setting influences the prokaryotic community and metabolome in deep-sea sponges. *Scientific Reports*, *12*(1), 3356. https://doi.org/10.1038/s41598-022-07292-3

Takasu, H., & Nagata, T. (2015). High Proline Content of Bacteria-Sized Particles in the Western North Pacific and Its Potential as a New Biogeochemical Indicator of Organic Matter Diagenesis. *Frontiers in Marine Science*, *Volume 2-2015*. https://doi.org/10.3389/fmars.2015.00110

Tanioka, T., Garcia, C. A., Larkin, A. A., Garcia, N. S., Fagan, A. J., & Martiny, A. C. (2022). Global patterns and predictors of C:N:P in marine ecosystems. *Communications Earth & Environment*, *3*(1), 271. https://doi.org/10.1038/s43247-022-00603-6

Tett, P., Droop, M. R., & Heaney, S. I. (1985). The Redfield Ratio and Phytoplankton Growth Rate. *Journal of the Marine Biological Association of the United Kingdom*, *65*(2), 487–504. https://doi.org/10.1017/S0025315400050566

Wanninkhof, R., Park, G.-H., Takahashi, T., Feely, R. A., Bullister, J. L., & Doney, S. C. (2013). Changes in deep-water CO2 concentrations over the last several decades determined from discrete pCO2measurements. *Deep Sea Research Part I: Oceanographic Research Papers*, *74*, 48–63. https://doi.org/10.1016/j.dsr.2012.12.005

Yoo, H. C., Yu, Y. C., Sung, Y., & Han, J. M. (2020). Glutamine reliance in cell metabolism. *Experimental & Molecular Medicine*, *52*(9), 1496–1516. https://doi.org/10.1038/s12276-020-00504-8